Photosensitized Breakage and Damage of DNA by CdSe−ZnS Quantum Dots

AbdulAziz Anas,[‡] Hidetaka Akita,[§] Hideyoshi Harashima,[§] Tamitake Itoh,[‡] Mitsuru Ishikawa,[‡,⊥,†] and Vasudevanpillai Biju*[,‡,⊥]

Nanobioanalysis Team, Health Technology Research Center, National Institute of Advanced Industrial Science and Technology (AIST), 2217-14 Hayashi-cho, Takamatsu, Kagawa 761-0395, Japan, and Graduate School of Pharmaceutical Sciences, Hokkaido University, Kita-Ku, Sapporo, Hokkaido 060-0812, Japan

Received: March 3, 2008; Revised Manuscript Received: May 23, 2008

Strand breakages and nucleobase damages in plasmid DNA (pDNA) by CdSe−ZnS quantum dots (QDs) are investigated under different conditions of photoactivation. Here, streptavidin functionalized CdSe−ZnS QDs are conjugated to biotinylated pDNA, and photosensitized strand breakages and nucleobase damages in the conjugates are investigated using atomic force microscopy (AFM) imaging, gel electrophoreses analyses, and assay of reactive oxygen intermediates (ROI). Also, reactions of photoactivated pDNA−QD conjugates with base excision repair enzymes such as formamidopyrimidine glycosylase (Fpg) and endonuclease III (Endo III) show damages of purine and pyrimidine bases. The base excision repair enzymes recognize and remove the damaged bases. The base excision reactions of photoactivated pDNA−QD conjugates resulted in pDNA strand breakages, which appeared as sheared bands in agarose gel images. On the basis of AFM imaging, reactions of Fpg and Endo III with damaged pDNA, ROI assay, and literature reports, we attribute the breakage and damage of pDNA to its reactions with ROI. The production of ROI by photoactivated QDs is confirmed by nitroblue tetrazolium (NBT) assay. The current work shows that photoactivation of QD-conjugated nucleic acids for an extended period of time is not favorable for their stability. On the other hand, photoinduced production of ROI by QDs is an emerging research area with potential applications in the photodynamic therapy of cancer. In this regard, photosensitized damage of pDNA observed in the current work shows possibilities of QDs in nucleus-targeted photodynamic therapy.

Introduction

Quantum confinement of excitons provides size-tuneable absorption and photoluminescence properties of semiconductor quantum dots (QDs). Additionally, the brightness and stability of photoluminescence and broad absorption and narrow photoluminescence bands make QDs superior to organic dyes and promising for biolabeling, bioanalysis/imaging, and therapeutic interventions.[1–18] Bruchez et al.[19] and Chan and Nie[20] introduced QDs to biology. Initially, there were some impediments in accepting QDs as biolabels due to their large size,[2] poor photoluminescence quantum efficiencies,[19,21,22] intrinsic blinking,[23–26] hydrophobic nature,[27] technical difficulties in conjugating QDs to biomolecules,[28] and lack of commercial availability. Recently, with the advancements in the synthesis of high-quality and surface-modified QDs,[19–21,29–31] QDs gained wide acceptance as bright and stable biolabels for multiplexed detection and multiphoton imaging both in vivo and in vitro. For example, the syntheses of highly luminescent QDs with surface functionalities such as amino (−NH_2),[32,33] carboxylic acid (−COOH),[34–37] and mercapto (−SH)[20,38–40] groups are well established. In 2002, Goldman et al.[41] prepared a QD-conjugated antibody by reacting QD−avidin bioconjugates with a biotinylated antibody. Avidin-conjugated QDs are promising biolabels because of their ability to label any biotinylated molecule/system such as proteins, DNA, and cell organelles via simple avidin−biotin linkage. Among different QDs available for various biological applications, CdSe−ZnS QDs are specifically attractive based on straightforward synthesss, size-tuneable photoluminescence throughout the visible region, and feasibility of bioconjugation via disulfide linkage on ZnS shells. Although bioconjugated QDs and their in vitro applications are widely accepted, extension of QDs toward in vivo applications is limited by concerns of their toxicity.[42–47]

The toxicity of QDs is broadly classified into chemically induced and photoinduced toxicities. Cadmium and selenium, the two constituents of CdSe QDs, are known to cause acute and chronic toxic effects in vertebrates and are of considerable human health and environmental concerns.[7,48] In a living cell, cadmium ions are taken up through calcium channels in the plasma membrane and accumulate intracellularly by binding with cytoplasmic and nuclear materials.[49] At cytotoxic levels, cadmium inhibits the biosyntheses of DNA, RNA, and protein, and it induces lipid peroxidation, DNA strand breakage, and chromosomal aberration.[50–52] On the other hand, selenium is a trace element essential for the syntheses of selenoproteins;[53] however, at elevated levels, selenium induces DNA damage, cell membrane perturbations, and oxygen stress.[54] The toxic effects of CdTe QDs due to the release of Cd^{2+} on the metabolic activities of cells were investigated by Cho et al.[55] Derfus et al. investigated the cytotoxicity of core-only CdSe QDs and core−shell QDs with different shell materials.[43] They reported 6−126 ppm concentrations of free Cd^{2+} in a 0.25 mg/mL CdSe QD solution. One of the main reasons of the release of Cd^{2+} from CdSe QDs is their surface oxidation. Therefore, the toxicity of CdSe QDs due to the release of Cd^{2+} can be considerably

* To whom correspondence should be addressed. E-mail: v.biju@aist.go.jp. Phone: (81) 87-869-3558. Fax: (81) 87-869-4113.
‡ AIST.
§ Hokkaido University.
† E-mail: ishikawa-mitsuru@aist.go.jp.
⊥ Also at Center for Arthropod Bioresources and Biotechnology, Kerala University, Kariavattom, Trivandrum, India.

10.1021/jp8018606 CCC: $40.75
Published on Web 06/26/2008

suppressed by overlaying protective shells. Ipe et al. identified a relation between surface coating and the release of Cd^{2+} by measuring photoinduced generation of free radicals of 5,5-dimethyl-1-pyrroline *N*-oxide in the presence of CdS, CdSe, and CdSe−ZnS QDs.[56] Here, the free radicals were generated by Cd^{2+}, and a complete suppression of the radical generation was achieved by overlaying ZnS shells on CdSe QDs. However, Green and Howman found the release of Cd^{2+} from biotin-functionalized CdSe−ZnS core−shell QDs and Cd^{2+}-induced damage of double-stranded DNA even in the dark.[42] Although there are several reports on the toxicity of QDs with reference to the release of Cd^{2+}, less is known about the toxicity due to selenium and photoactivation. While the toxicity due to the release of cadmium and selenium ions is controlled by physically protecting the CdSe core, photoinduced toxicity as a result of the production of reactive oxygen intermediates (ROI) is not investigated in detail. The photoinduced toxicity due to the production of ROI is less controlled as it is a barrierless process which is initiated by resonance energy transfer from QDs to molecular oxygen.[14,15]

Reactive oxygen intermediates are highly reactive species such as singlet oxygen ($^1O_2$), superoxide anion ($O_2^{-\bullet}$), hydroxyl radical ($HO^\bullet$), and hydrogen peroxide (H_2O_2), which are formed by the activation/reduction of molecular oxygen.[57] In a biological system, ROI are considered to be toxic byproducts of cellular metabolism and are involved in signal transduction and prevention of pathogen invasion.[58] A minimum concentration of ROI is essential for maintaining the regular metabolism of cells. Also, reactive oxygen scavenging mechanisms are operative in cells for self-protection from ROI-mediated toxicity.[59,60] However, elevated levels of ROI induce double-strand breakages and nucleobase damages in DNA.[61]Photoinduced production of ROI is initiated by a nonradiative energy transfer from a photoactivated/photosensitized chromophore to molecular oxygen in the ground state. This nonradiative energy transfer generates highly reactive $^1O_2$ which, in turn, initiates the production of other ROI by reacting with water and other molecules in the environment.[27] A similar mechanism is pertinent in the production of ROI by photoactivated QDs.[14,15,42,44,62]

Here, we conjugated streptavidin-functionalized QDs to biotinylated pDNA and investigated the photoinduced toxic effects of QDs on pDNA using agarose gel electrophoresis, AFM imaging, and DNA damage assays. We used formamidopyrimidine glycosylase (Fpg) and endonuclease III (Endo III) enzymes in the DNA damage assays. Also, the productions of ROI by QDs are examined in the dark, in the absence and presence of oxygen, and under laser excitation. Finally, the photosensitized strand breakages and nucleobase damages in pDNA are correlated with photoinduced production of ROI, which is estimated based on the conversion of yellowish nitroblue tetrazolium (NBT) chloride into purple formazan derivatives.

Experimental Section

Materials and Samples. Streptavidin-functionalized QDs with photoluminescence of $\lambda_{max} \sim 585$ and 605 nm, SYBR gold nucleic acid stain, and biotinylated pDNA (pcDNA 3.1) were obtained from Invitrogen, U.S.A. Nitroblue tetrazolium (NBT) chloride was obtained from Sigma, and base excision repair enzymes Fpg and Endo III were obtained from Trevigen, U.S.A. All other chemicals including 2-amino-2-(hydroxymethyl)-1,3-propanediol hydrochloride (Tris-HCl), disodium salt of ethylenediaminetetraacetic acid (EDTA), (*N*-[2-hydroxyethyl]piperazine-*N*′-[2-ethanesulfonic acid]) (HEPES), acetic acid, and agarose were obtained from Aldrich.

We prepared pDNA−QD conjugates by reacting biotinylated pDNA (10 μg/mL) with 0.5 nM (0.5 and 1 nM in AFM experiments) streptavidin-functionalized QDs in HEPES buffer for 30 min. The conjugate solution was aliquoted into three equal portions. The first portion was incubated at 25 °C in the dark for 1 h, the second portion was exposed to a 532 nm laser ($\sim$1 W/cm^2, Nd: YVO_4, Spectra Physics Millennia IIs) or a 400 nm laser ($\sim$1 W/cm^2, Coherent OPA) for 1 h, and the third portion was used as a control. The effects of QDs on pDNA under the above conditions were examined by agarose gel electrophoreses and AFM imaging. Samples for electrophoreses were prepared by mixing 10 μL of pDNA−QD conjugates with the gel loading buffer (0.04 M Tris acetate and 1 mM EDTA, TAE). Samples for AFM imaging were prepared by mixing 1 μL of pDNA−QD conjugate with 5 nM $MgCl_2$, spreading on freshly cleaved mica sheets and incubating for 5 min at room temperature. The sample surfaces were gently washed with deionized water before AFM imaging.

Instruments and Methods. Electrophoresis was carried out using a PowerPac Basic electrophoretic apparatus (BioRad, U.S.A.). Tapping-mode AFM images were collected using a MFP-3D microscope (Asylum Research, Santa Barbara, CA) equipped with ultra sharp (radius of curvature < 10 nm) nanoprobes (Olympus, Japan). The cantilevers used were 160 μm long, had a spring constant of 42 N/m, and had a resonance frequency of $\sim$360 kHz. Absorption spectra were recorded using a U4100 Hitachi spectrophotometer. Details of photoluminescence lifetime measurements are reported elsewhere;[25] simply, we used a combination of a polychromator (Chromex, model 250IS), a photon-counting streak-scope (Hamamatsu, model C4334), and 400 nm pulses (150 fs) from an optical parametric amplifier (Coherent OPA 9400).

Strand breakage of pDNA was examined using agarose gel electrophoresis. Photoactivated pDNA−QD conjugate solutions (10 μL each) were mixed with the gel loading buffer and loaded into wells in 1% agarose gel, which was immersed in the electrophoresis buffer in a horizontal tank. Electrophoresis was run at 75 V for 90 min. SYBR gold nucleic acid stain was incorporated along with the gel. After electrophoresis, the gel was placed on a UV transilluminator, and DNA bands were photographed with a digital camera (Olympus, Japan). Nucleobase damage of pDNA was examined using Fpg and Endo III enzymes. For this, a solution of pDNA−QD conjugates was photoactivated at 532 or 400 nm for 1 h followed by incubating at 37 °C for 30 min in two portions with Fpg and Endo III. The samples were loaded on 1% agarose gel, and electrophoresis was carried out in TAE buffer at 75 V for 90 min. Gel documentation was carried out as described above.

We evaluated the role of photoactivation of QDs on the strand breakage and nucleobase damages of pDNA by measuring the production of ROI by QDs at 15 min intervals for 1 h under three conditions such as incubation in the dark, exposure to a 532 nm laser beam in the presence of oxygen, and exposure to a 532 nm laser beam after purging with nitrogen gas. The production of ROI was evaluated in terms of the reduction of yellow NBT into purple formazan derivatives. This evaluation is widely known as NBT assay in which the optical density of formazan derivatives is measured at 650 nm. In a typical assay, a solution of QDs (0.5 nM) and NBT (100 μM) was prepared in a 1:1 water/DMSO mixture, and the solution was incubated under the conditions mentioned above.

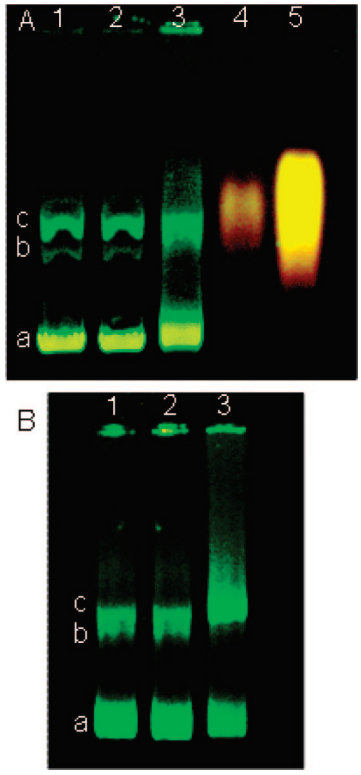

Figure 1. Agarose gel electrophoreses images of pDNA and pDNA−QD conjugates: (A) gel image of pDNA before (lane 1) and after photoactivation (lane 2), pDNA−QD conjugates before photoactivation (lane 3), and CdSe−ZnS QDs (lane 4, 0.5 nM; lane 5, 5 nM). (B) Gel images of pDNA−QD conjugates: (lane 1) as-prepared sample, (lane 2) incubated in the dark for 1 h, and photoactivated at 400 nm for 1 h (lane 3). (a) Supercoiled, (b) circular, and (c) linear conformers of pDNA.

Results and Discussion

We characterized the formation of pDNA−QD conjugates and the photosensitized breakage and damage of the conjugates using agarose gel electrophoresis and AFM imaging. Figure 1 shows agarose gel images of pDNA with and without QD conjugation and before and after photoactivation. Lanes 1 and 3 in Figure 1A are the gel images of pDNA before and after QD conjugation. The different bands in lane 1 correspond to supercoiled (a), circular (b), and linear (c) conformations of pDNA. Also, lanes 4 and 5 in Figure 1A are the gel images of low (5 nM) and high (50 nM) concentrations of QDs. On the basis of lanes 1 and 3 in Figure 1A, it is apparent that the formation of pDNA−QD conjugates is associated with a slight decrease in the electrophoretic mobility of pDNA. It may be noted that the electrophoretic mobility of QDs is slightly lower than that of pDNA. Probably, the relatively low mobility of QDs (lanes 4 and 5 in Figure 1A) is the origin of the difference in the gel image of pDNA before and after conjugation with QDs. Interestingly, we observed a considerable shearing of various bands in the gel image of photoactivated pDNA−QD conjugates. Also, the intensity of the supercoiled conformer was considerably decreased with a corresponding increase in the intensity of a band migrating behind that. The band migrating behind the supercoiled pDNA includes damaged circular and linear conformers; the circular and linear conformers are formed by the strand breakages and nucleobase damages of the supercoiled conformer. Lanes 1 and 3 in Figure 1B are the gel images of pDNA−QD conjugates before and after 1 h of photoactivation at 400 nm (1 W/cm^2). The shearing of the gel

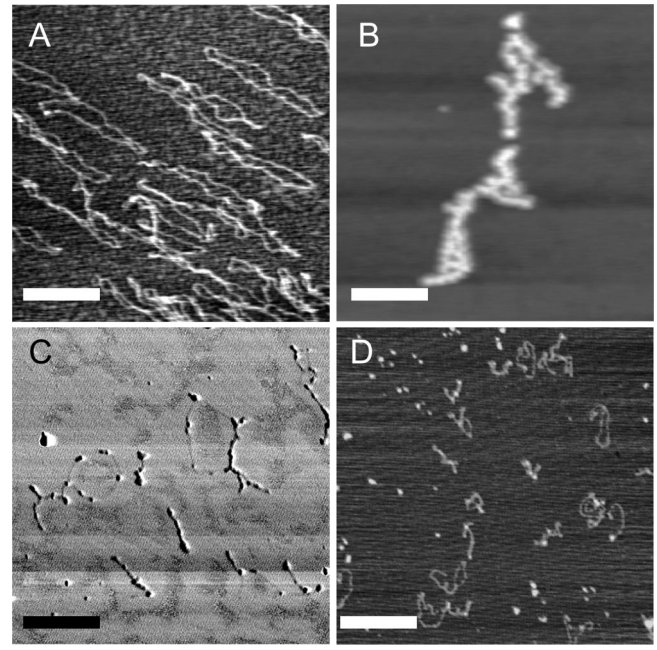

Figure 2. AFM images of pDNA and pDNA−QD conjugates: (A) biotinylated pDNA before QD conjugation, (B) pDNA with ∼200 biotin moieties after conjugation with QDs, (C) pDNA with ∼20 biotin moieties after conjugation with QDs, and (D) pDNA with ∼20 biotin moieties after conjugation with QDs followed by photoactivation at 532 nm for 1 h. The scale bars are (A) 800 nm, (B) 400 nm, (C) 600 nm, and (D) 500 nm.

image and the decrease in the intensity of the supercoiled conformer in a photoactivated pDNA−QD sample are attributed to photosensitized breakage and damage of pDNA. On the other hand, the gel image pDNA−QD conjugates kept in the dark (lane 2 in Figure 1B) and that of photoactivated pDNA without QD conjugation (lane 2 in Figure 1A) are essentially not affected. These results show that the strand breakages and nucleobase damages of DNA are not spontaneous processes but result from photosensitized reactions between DNA and QDs.

The formation of pDNA−QD conjugates and the photosensitized strand breakage of pDNA are further characterized by AFM imaging. We reacted biotinylated pDNA having different densities of biotin with QD solutions of different concentrations and found that the density of QDs on pDNA is directly related to the number of biotin units and the concentrations of QD solutions. Figure 2A is the AFM image of a biotinylated pDNA sample. Figure 2B and C shows the AFM images of pDNA−QD conjugates prepared by reacting pDNA with ∼200 (Figure 2B) and ∼20 (Figure 2C) biotin units with 1 nM QD solutions. The high and the low densities of QDs on pDNA in Figure 2B and C shows that the pDNA−QD conjugates are formed by streptavidin−biotin linkage and not by nonspecific interactions between pDNA and QDs. Also, aggregation of pDNA was minimized in conjugates prepared from pDNA with ∼20 biotin units and low concentrations (≤1 nM) of QD solutions (Figure S1, Supporting Information). The strand breakage in photoactivated pDNA−QD conjugates was confirmed from AFM images. For this, we selected pDNA−QD conjugates with a low density of QDs (<20 QDs/pDNA) and photoactivated at 532 nm (1 W/cm^2) for 1 h. Figure 2C and D shows the AFM images of pDNA−QD conjugates before and after the photoactivation. We observed circular and supercoiled pDNA−QD conjugates before photoactivation (Figure 2C and Figure S1) and fragmented pDNA−QD conjugates after the photoactivation (Figure 2D). We attribute the strand breakage of pDNA−QD

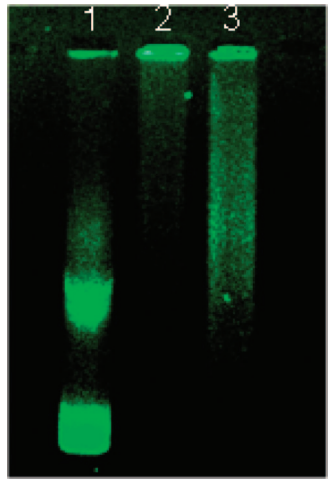

Figure 3. Agarose gel image of pDNA−QD conjugates: (lane 1) before photoactivation, (lane 2) after photoactivation and reaction with Fpg, and (lane 3) after photoactivation and reaction with Endo III. The photoactivated pDNA−QD samples were incubated with the enzymes for 30 min at 37 °C before loading in the gel.

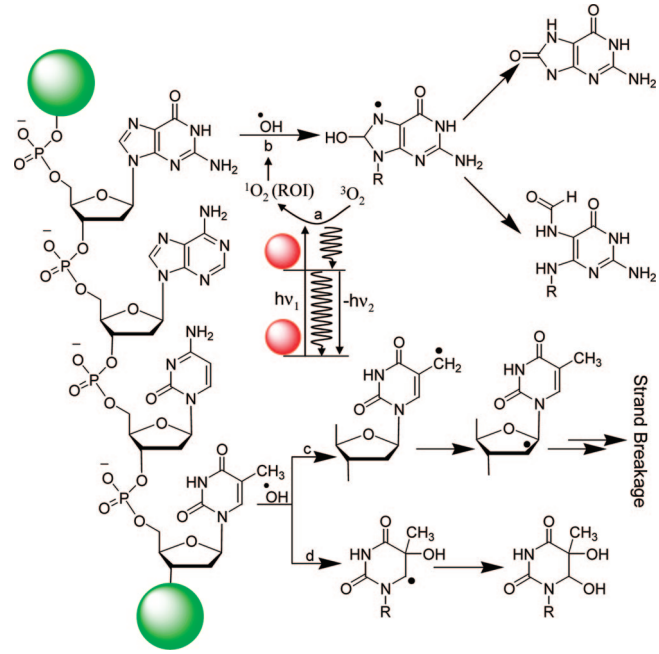

Figure 4. Schematic presentation of (a) the photoinduced production of ROI by QDs, (b, d) the damages of nucleobases by ROI, and (c) hydrogen abstraction by ROI and DNA strand breakage.

conjugates to the reactions of ROI with pDNA. Specifically, the generation of $^1O_2$ via energy transfer from photoactivated QDs to molecular oxygen, conversion of $^1O_2$ into HO•, and the abstraction of a hydrogen atom from the ribosyl group of pDNA are the possible origins of the DNA strand breakage. We consider this possibility based on an estimation of ROI production by photoactivated QDs, the mechanism of conversion of $^1O_2$ into HO• and other ROI, and literature reports on DNA double-strand breakages by hydrogen atom abstraction.[61,63–65] Also, the photosensitized DNA strand breakage is supported by control experiments in which the breakage was absent without photoactivation of pDNA−QD conjugates and without conjugation of QDs to pDNA.

The photosensitized nucleobase damages in pDNA are further characterized using reactions of base excision repair enzymes with photoactivated pDNA−QD conjugates. In addition to the photosensitized strand breakages in pDNA-QD conjugates, as observed in the AFM image (Figure 2D), we found considerable damages of purine and pyrimidine bases. Figure 3 shows an agarose gel image of photoactivated pDNA−QD conjugates followed by reactions with base excision repair enzymes such as Fpg (lane 2) and Endo III (lane 3). The pDNA−QD samples were photoactivated at 400 nm (1 W/cm^2) for 1 h. The electrophoretic migration of photoactivated pDNA−QD conjugates is considerably decreased, and the bands are sheared after incubations with Fpg and Endo III. On the other hand, no such changes were observed for pDNA−QD conjugates kept in the dark. The shearing of the bands of photoactivated pDNA−QD conjugates is due to the excision of damaged bases by the enzymes and breakage of DNA.[64,66,67] Fpg specifically reacts with damaged guanine bases such as 2,6-diamino-5-formamido-4-hydroxygunanine (FAPyG) and 8-oxoguanosine (8-oxo-G), and Endo III is specific to oxidized pyrimidines and apurinic sites. It is widely known that ROI such as $^1O_2$ and HO• induce base modifications in DNA.[68] Therefore, the sheared bands in the gel image (lanes 2 and 3 in Figure 3) confirm the nucleobase damages in photoactivated pDNA−QD conjugates. The production of ROI is confirmed by NBT assay, which is discussed below.

The electrophoresis data, AFM images, and enzymatic reactions show strand breakages and nucleobase damages in photoactivated pDNA−QD conjugates. We correlate the breakage and damage of DNA with the production of $^1O_2$ and HO• by photoactivated QDs. The strand breakage takes place when a radical center is created in the ribosyl group of DNA. The ribosyl-centered radicals are generated by either a direct abstraction of a hydrogen atom from the ribose moiety by HO• or an abstraction of a hydrogen atom from the methyl group of thymine by HO• followed by a hydrogen atom transfer from the ribosyl group to the thymine radical.[61,65] The ribose-centered radicals eventually cleave the phosphate−ribose bond and break the DNA strand. The hydrogen atom abstraction and the strand breakage in DNA are schematically presented in Figure 4 (path c). Additional routes of strand breakages in photoactivated and enzyme-treated pDNA−QD conjugates are initiated by the excision of damaged nucleobases via the hydrolysis of the glycosidic bond and elimination of phosphate groups.[69]

The damages of purine and pyrimidine bases by ROI and the detection of the damages using the base excision repair enzymes Fpg and Endo III are well-documented in photobiology.[64,69] Here, we consider two possibilities for the damage of guanine nucleobase, one initiated by $^1O_2$ and the other by HO•. In the former case, an electron transfer between a guanine nucleobase and $^1O_2$ creates a guanine cation radical which, upon subsequent reactions, produces 8-hydroxyguanine nucleoside. In the latter case, a direct addition of a HO• at the C8 position of a guanine nucleobase produces 8-hydroxyguanine nucleobase with an N7-centered radical which subsequently rearranges into 8-oxo-guanine (8-oxo-G) or 2,6-diamino-5-formamido-4-hydroxyguanine (FAPyG). In the current work, we attribute the pDNA damages to the reactions of guanine with HO• and the formation of 8-oxo-G and FAPyG (path b in Figure 4). This path of the nucleobase damage is substantiated by the reactions of Fpg with FAPyG and 8-oxo-G and the sheared band in the gel image (lane 2 in Figure 3). Also, several other products are known from the reactions between ROI and DNA.[70] Therefore, in the current work, the photosensitized damages of pDNA−QD conjugates originate from the reactions of $^1O_2$ and HO• with nucleobases. Like guanine, pyrimidines also react with HO• and form various hydroxylated derivatives such as thymine glycol,

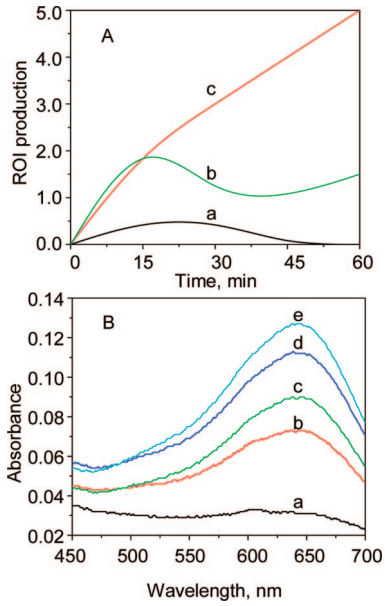

Figure 5. NBT assay of ROI production by QDs (photoluminescence λ_{max} = ~600 nm). (A) Temporal evolution of the optical density at 650 nm of NBT−QD mixtures (a) incubated in the dark, (b) photoactivated (0.1 W/cm^2 at 532 nm) after purging nitrogen gas, and (c) photoactivated (0.1 W/cm^2 at 532 nm) in the presence of oxygen. (B) Absorption spectra of a mixture of QDs and NBT in a 1:1 DMSO/water mixture under photoactivation (0.1 W/cm^2 at 532 nm) for (a) 0, (b) 15, (c) 30, (d) 45, and (e) 60 min. The increase in the optical density corresponds to the production of ROI and the conversion of NBT into formazan derivatives.

uracil glycol, and 5-hydroxy-5,6-dihydrothymine.[65] For example, the addition of HO$^\bullet$ to the C5═C6 double bond in thymine followed by the formation of a C6-centered radical is shown in Figure 4 (path d). The C6-centered radical reacts further with a second HO$^\bullet$ and forms thymine glycol. It is widely known that Endo III recognizes and excises such damaged pyrimidines.[69] The sheared band in the gel image (lane 3 in Figure 3) confirms the reactions of Endo III with the damaged pyrimidines. Therefore, reactions of HO$^\bullet$ with pyrimidines are also involved in the photosensitized damage of pDNA.

We characterized the production of ROI by photoactivated QDs using NBT assay. NBT assay involves spectrophotometric measurements of the reduction of yellowish NBT into purple formazan derivatives by ROI. The reduction of NBT by ROI into mono- and diformazan derivatives results in an increase of absorbance in the 450−700 nm range. Therefore, spectrophotometric measurement of the formation of formazan derivatives is a standard method to quantify the production of ROI.[71–73] Figure 5A shows the production of ROI by aqueous solutions (1:1 water/DMSO mixture) of QDs with (trace c) and without (trace a) photoactivation and in the presence (trace c) and absence (trace b) of oxygen. Here, the solutions of QDs and NBT were photoactivated at 532 nm for 1 h, and the optical densities at 650 nm were measured at 15 min intervals. The photoactivation of QDs in the presence of NBT resulted in a broad absorption in the 450−700 nm region (Figure 5B), the intensity of which increased with time under photoactivation. The broad absorption band is characteristic of formazan derivatives. ROI production was not estimated by exciting the QD−NBT samples at 400 nm because of a residual absorption of NBT extending to the 400 nm region. Also, we examined the production of ROI by QDs in organic phases. For example, NBT assay of ROI production by a solution of CdSe−ZnS QDs (photoluminescence λ_{max} ~ 600 nm) in chloroform is shown in

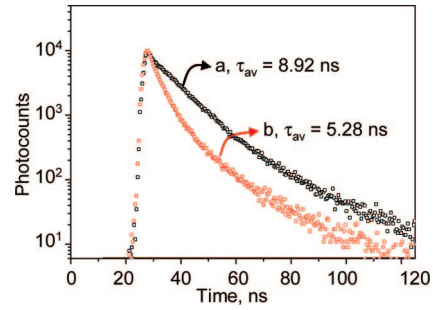

Figure 6. Photoluminescence decay profiles of QDs in the presence (a) and absence (b) of oxygen. Photons were collected through a band-pass filter for QD605.

Figure S2 (Supporting Information). We observed a continuous increase of absorbance due to the formation of formazan derivatives; however, the absorption spectra are blue-shifted compared to that of QD−NBT in water/DMSO mixtures. These results show an increase in the production of ROI by QDs with time under photoactivation. On the other hand, NBT remained unchanged in nitrogen-purged solutions and solutions kept in the dark. Similarly, breakage and damage were absent in pDNA−QD conjugates kept in the dark. Therefore, we attribute the reduction of NBT into formazan derivatives and the damage and breakage of pDNA to the production of ROI by photoactivated QDs. The production of ROI is initiated by nonradiative energy transfer from photoactivated QDs to molecular oxygen, that is, quenching of the photoexcited state of QDs. To clarify the energy-transfer process, we examined the photoluminescence lifetimes of QD solutions in the presence and absence of oxygen. We found a considerable decrease in the photoluminescence lifetime of QDs in the absence of oxygen; indeed, an increase is expected. Figure 6 shows the photoluminescence decays and lifetimes of QDs in the presence and absence of oxygen. Here, we consider two contradicting interactions of QDs with oxygen, (i) quenching of the photoexcited state by energy transfer to molecular oxygen[14] followed by the production of $^1O_2$ and other ROI and (ii) enhancement of the photoluminescence quantum efficiency and lifetime via surface passivation.[74,75] The efficiency of the former process is only ~5%, while in the latter case, the photoluminescence quantum efficiency of QDs increases by a factor 10 or more. Therefore, in the current work, the overall decrease in the photoluminescence lifetime of QDs in the absence of oxygen is dominated by the suppression of the surface passivation effect. Yet, another possibility for the breakage and damage of pDNA is direct chemical reactions with Cd^{2+}, which is released from QDs. It is known that the binding of Cd^{2+} at guanine sites in the major grooves of DNA results in nucleobase damages.[51,52] Also, in the presence of H_2O_2, Cd^{2+} produces HO$^\bullet$ which, in turn, induces DNA breakage and damage by the abstraction of hydrogen atoms.[50] Nevertheless, the release of Cd^{2+} is the primary requirement for such chemically induced breakage and damage of DNA. The release of Cd^{2+} by core−shell QDs depends on the thickness as well as whether the shells are complete or not. In the current work, we ruled out the involvement of Cd^{2+} in the breakage and damage of pDNA by selecting CdSe−ZnS QDs with additional polymer shells. Also, we ruled out the release of Cd^{2+} from QDs on the basis of negligible ROI production and the absence of breakage and damage of pDNA in the dark. Therefore, we attribute the breakage and damage of pDNA−QD conjugates to the photoinduced production of ROI by QDs and the reactions of ROI with pDNA.

Conclusions

The current work shows strand breakages and nucleobase damages in pDNA by ROI, which is produced by photoactivated QDs. Photoactivated QDs nonradiatively transfer energy to proximal molecular oxygen and produce $^1O_2$ which, in turn, produces other ROI such as the superoxide anion, $HO^{\bullet}$, and hydrogen peroxide (H_2O_2). Among these, ROI, $^1O_2$ and $HO^{\bullet}$ induce strand breakage and nucleobase damages in DNA by the abstraction of hydrogen atoms from nucleobases and ribosyl groups. The production of ROI was confirmed by NBT assay, and the breakage and damage of DNA were characterized using AFM imaging and gel electrophoresis. The photoinduced production of $^1O_2$ by QDs is an emerging research area with potential applications in the photodynamic therapy of cancer. Samia et al.[14] investigated the production of $^1O_2$ by photoactivated CdSe−ZnS QDs in toluene solutions, and the efficiency was estimated to be only ∼5%. This low efficiency of $^1O_2$ production shows that a direct energy transfer from QDs to molecular oxygen is not efficient. More recently, Tsay et al.[62] investigated photoinduced energy-transfer processes from QDs to potential photosensitizers such as rose bengal and chlorin e6. They achieved ∼50% efficiency of energy transfer, which is promising to improve the production of ROI and applications of QDs in photodynamic therapy. The production of ROI by QDs and ROI-induced breakage and damage of DNA in the current work shows possibilities of QDs in nucleus-targeted photodynamic therapy. Previously, Liang et al. observed damages of ctDNA under UV light irradiation in the presence of water-soluble CdSe QDs.[44] Although the origin of the damage of DNA was attributed to the reactions of ROI with DNA, the direct UV effect on DNA cannot be completely neglected. In the current work, pDNA−QD conjugates are photoactivated at 400 or 532 nm, and therefore, the breakage and damage of DNA are solely attributed to the reactions of ROI with DNA. An extension of the current work on photosensitized breakage and damage of DNA with a combination of NIR QDs/multiphoton excitation and nucleus targeting of QD-photosensitizer hybrids in cancer cells/tumors would considerably affect the photodynamic therapy of cancer.

Acknowledgment. This work is supported by a Seed Research Fund and a Special Coordination Fund for Promoting Science and Technology of the Ministry of Education, Culture, Sports, Science, and Technology, the Japanese Government.

Supporting Information Available: AFM image of pDNA−QD conjugates and absorption spectra of formazan derivatives in chloroform. This material is available free of charge via the Internet at http://pubs.acs.org.

References and Notes

(1) Alivisatos, P.; Gu, W.; Larabell, C. *Annu. Rev. Biomed. Eng.* **2005**, *7*, 55.
(2) Bailey, R. E.; Smith, A. M.; Nei, S. *Physica E* **2004**, *25*, 1.
(3) Biju, V.; Muraleedharan, D.; Nakayama, K.; Shinohara, Y.; Itoh, T.; Baba, Y.; Ishikawa, M. *Langmuir* **2007**, *23*, 10254.
(4) Caruthers, S. D.; Wickline, S. A.; Lanza, G. M. *Curr. Opin. Biotechnol.* **2007**, *18*, 1.
(5) Chan, W. C. W.; Maxwell, D. J.; Gao, X. H.; Bailey, R. E.; Han, M. Y.; Nie, S. M. *Curr. Opin. Biotechnol.* **2002**, *13*, 40.
(6) Giepmans, B. N. G.; Adams, S. R.; Ellisman, M. H.; Tsien, R. Y. *Science* **2006**, *312*, 217.
(7) Hardman, R. *Environ. Health. Perspect.* **2006**, *114*, 165.
(8) Jaiswal, J. K.; Goldman, E. R.; Mattoussi, H.; Simon, S. M. *Nat. Methods.* **2004**, *1*, 73.
(9) Jamieson, T.; Bakhshi, R.; Petrova, D.; Pocock, R.; Imani, M.; Seifalian, A. M. *Biomaterials* **2007**, *28*, 4717.
(10) Medintz, I. L.; Uyeda, H. T.; Goldman, E. R.; Mattoussi, H. *Nat. Mater.* **2005**, *4*, 435.
(11) Michalet, X.; Pinaud, F. F.; Bentolila, L. A.; Tsay, J. M.; Doose, S.; Li, J. J.; Sundaresan, G.; Wu, A. M.; Gambhir, S. S.; Weiss, S. *Science* **2005**, *307*, 538.
(12) Parak, W. J.; Pellegrino, T.; Plank, C. *Nanotechnology* **2005**, *16*, R9.
(13) Pinaud, F.; Michalet, X.; Bentolila, L. A.; Tsay, J. M.; Doose, S.; Li, J. J.; Iyer, G.; Weiss, S. *Biomaterials* **2006**, *27*, 1679.
(14) Samia, A. C. S.; Chen, X. B.; Burda, C. *J. Am. Chem. Soc.* **2003**, *125*, 15736.
(15) Samia, A. C. S.; Dayal, S.; Burda, C. *Photochem. Photobiol.* **2006**, *82*, 617.
(16) Smith, A. M.; Nie, S. M. *Analyst* **2004**, *129*, 672.
(17) Zhou, M.; Ghosh, I. *Biopolymers* **2007**, *88*, 325.
(18) Prasad, P. N. *Mol. Cryst. Liq. Cryst.* **2006**, *446*, 1.
(19) Bruchez, J. M.; Moronne, M.; Gin, P.; Weiss, S.; Alivisatos, P. *Science* **1998**, *281*, 2013.
(20) Chan, W. C. W.; Nie, S. *Science* **1998**, *281*, 2016.
(21) Murray, C. B.; Norris, D. J.; Bawendi, M. G. *J. Am. Chem. Soc.* **1993**, *115*, 8706.
(22) Jeong, S.; Achermann, M.; Nanda, J.; Ivanov, S.; Klimov, V. I.; Hollingsworth, J. A. *J. Am. Chem. Soc.* **2005**, *127*, 10126.
(23) Nirmal, M.; Dabbousi, B. O.; Bawendi, M. G.; Macklin, J. J.; Trautman, J. K.; Harris, T. D.; Brus, L. E. *Nature* **1996**, *383*, 802.
(24) Biju, V.; Makita, Y.; Nagase, T.; Yamaoka, Y.; Yokoyama, H.; Baba, Y.; Ishikawa, M. *J. Phys. Chem. B* **2005**, *109*, 14350.
(25) Matsumoto, Y.; Kanemoto, R.; Itoh, T.; Nakanishi, S.; Ishikawa, M.; Biju, V. *J. Phys. Chem. C* **2008**, *112*, 1345.
(26) Kuno, M.; Fromm, D. P.; Hamann, H. F.; Gallagher, A.; Nesbitt, D. J. *J. Chem. Phys.* **2001**, *115*, 1028.
(27) Yu, W. W.; Chang, E.; Drezek, R.; Colvin, V. L. *Biochem. Biophys. Res. Commun.* **2006**, *348*, 781.
(28) Klostranec, J.; Chan, W. *Adv. Mater.* **2006**, *18*, 1953.
(29) Katari, J.; Colvin, V.; Alivisatos, A. P. *J. Phys. Chem.* **1994**, *98*, 4109.
(30) Talapin, D. V.; Rogach, A. L.; Kornowski, A.; Haase, M.; Weller, H. *Nano Lett.* **2001**, *1*, 207.
(31) Tomasulo, M.; Yildiz, I.; Kaanumalle, S. L.; Raymo, F. M. *Langmuir* **2006**, *22*, 10284.
(32) Dubois, F.; Mahler, B.; Dubertret, B.; Doris, E.; Mioskowski, C. *J. Am. Chem. Soc.* **2007**, *129*, 482.
(33) Ballou, B.; Ernst, L. A.; Andreko, S.; Harper, T.; Fitzpatrick, J. A. J.; Waggoner, A. S.; Bruchez, M. P. *Bioconjugate Chem.* **2007**, *18*, 389.
(34) Dubertret, B.; Skourides, P.; Norris, D. J.; Noireaux, V.; Brivanlou, A. H.; Libchaber, A. *Science* **2002**, *298*, 1759.
(35) Mattheakis, L. C.; Dias, J. M.; Choi, Y.-J.; Gong, J.; Bruchez, M. P.; Liu, J.; Wang, E. *Anal. Biochem.* **2004**, *327*, 200.
(36) Ballou, B.; Lagerholm, B. C.; Ernst, L. A.; Bruchez, M. P.; Waggoner, A. S. *Bioconjugate Chem.* **2004**, *15*, 79.
(37) Kim, S.; Bawendi, M. *J. Am. Chem. Soc.* **2003**, *125*, 14652.
(38) Srinivasan, C.; Lee, J.; Papdimitrakopoulos, F.; Silbart, L. K.; Zhao, M.; Burgess, D. J. *Mol. Ther.* **2006**, *14*, 192.
(39) Wu, S.-M.; Zhao, X.; Zhang, Z.-L.; Xie, H.-Y.; Tian, Z.-Q.; Peng, J.; Lu, Z.-X.; Pang, D.-W.; Xie, Z.-X. *ChemPhysChem* **2006**, *7*, 1062.
(40) Sun, Y. H.; Liu, Y. S.; Vernier, P. T.; Liang, C. H.; Chong, S. Y.; Marcu, L.; Gundersen, M. A. *Nanotechnology* **2006**, *17*, 4469.
(41) Goldman, E. R.; Balighian, E. D.; Mattoussi, H.; Kuno, M. K.; Mauro, J. M.; Tran, P. T.; Anderson, G. P. *J. Am. Chem. Soc.* **2002**, *124*, 6378.
(42) Green, M.; Howman, E. *Chem. Commun.* **2005**, *121*, 121.
(43) Derfus, A. M.; Chan, W. C. W.; Bhatia, S. N. *Nano Lett.* **2004**, *4*, 11.
(44) Liang, J.; He, Z.; Zhang, S.; Huanga, S.; Ai, X.; Yang, H.; Han, H. *Talanta* **2007**, *71*, 1675.
(45) Kirchner, C.; Liedl, T.; Kudera, S.; Pellegrino, T.; Javier, A. M.; Gaub, H. E.; Sto11zle, S.; Fertig, N.; Parak, W. J. *Nano Lett.* **2005**, *5*, 331.
(46) Lovric, J.; Cho, S. J.; Winnik, F. M.; Maysinger, D. *Chem. Biol.* **2005**, *12*, 1227.
(47) Mahtab, R.; Sealey, S.; Hunyadi, S.; Kinard, B.; Ray, T.; Murphy, C. *J. Inorg. Biochem.* **2007**, *101*, 559.
(48) Satarug, S.; Mooe, M. *Environ. Health Perspect.* **2004**, *112*, 1099.
(49) Beyersmann, D.; Hechtenberg, S. *Toxicol. Appl. Pharmacol.* **1997**, *144*, 247.
(50) Stohs, S. J.; Bagchi, D. *Free Radical Biol. Med.* **1995**, *18*, 321.
(51) Prakash, S.; Rao, S.; Dameron, C. *Biochem. Biophys. Res. Commun.* **1998**, *244*, 198.
(52) Hossain, Z.; Huq, F. *J. Inorg. Biochem.* **2002**, *90*, 85.
(53) Gu, Q. P.; Beilstein, M. A.; Vendeland, S. C.; Lugade, A.; Ream, W.; Whanger, P. D. *Gene* **1997**, *193*, 187.
(54) Shen, H.-M.; Yang, C.-F.; Ong, C.-N. *Int. J. Cancer* **1999**, *81*, 820.
(55) Cho, S. J.; Maysinger, D.; Jain, M.; Röder, B.; Hackbarth, S.; Winnik, F. M. *Langmuir* **2007**, *23*, 1974.

(56) Ipe, B. I.; Lehnig, M.; Niemeyer, C. M. *Small* **2005**, *1*, 706.
(57) Wiseman, H.; Halliwell, B. *Biochem. J.* **1996**, *313*, 17.
(58) Droge, W. *Physiol. Rev.* **2002**, *82*, 47.
(59) Luo, X.; Budihardjo, I.; Zou, H.; Slaughter, C.; Wang, X. *Cell* **1998**, *94*, 481.
(60) Su, M.; Yang, Y.; Yang, G. *FEBS Lett.* **2006**, *580*, 4136.
(61) Burrows, C. J.; Muller, J. G. *Chem. Rev.* **1998**, *98*, 1109.
(62) Tsay, J. M.; Trzoss, M.; Shi, L. X.; Kong, X. X.; Selke, M.; Jung, M. E.; Weiss, S. *J. Am. Chem. Soc.* **2007**, *129*, 6865.
(63) Sies, H. *Mutat. Res.* **1993**, *299*, 183.
(64) Epe, B. *Chem. Biol. Interact.* **1991**, *80*, 239.
(65) Cadet, J.; Delatour, T.; Douki, T.; Gasparutto, D.; Pouget, J. P.; Ravanat, J. L.; Sauvaigo, S. *Mutat. Res.* **1999**, *424*, 9.
(66) Demple, B.; Harrison, L. *Annu. Rev. Biochem.* **1994**, *63*, 915.
(67) Boiteux, S.; Gajewski, E.; Laval, J.; Dizdaroglu, M. *Biochemistry* **1992**, *31*, 106.
(68) Yu, T.-W.; Anderson, D. *Mutat. Res.* **1997**, *379*, 201.
(69) Cadet, J.; Bourdat, A.-G.; D'Ham, C.; Duarte, V.; Gasparutto, D.; Romieu, A.; Ravanat, J.-L. *Rev. Mutat. Res.* **2000**, *462*, 121.
(70) Gasparutto, D.; Bourdat, A.-G.; D'Ham, C.; Duarte, V.; Romieu, A.; Cadet, J. *Biochimie* **2000**, *82*, 19.
(71) Goodwin, D. C.; Aust, S. D.; Grover, T. A. *Chem. Res. Toxicol.* **1996**, *9*, 1333.
(72) Blelski, J.; Shiue, G. G.; Bajuk, S. *J. Phys. Chem.* **1980**, *84*, 830.
(73) Kovacs, A.; Baranyai, M.; Wojnarovits, L.; Moussa, A.; Othman, I.; McLaughlin, W. *Radiat. Phys. Chem.* **1999**, *55*, 799.
(74) Biju, V.; Kanemoto, R.; Matsumoto, Y.; Ishii, S.; Nakanishi, S.; Itoh, T.; Baba, Y.; Ishikawa, M. *J. Phys. Chem. C* **2007**, *111*, 7924.
(75) Myung, N.; Bae, Y.; Bard, A. J. *Nano Lett.* **2003**, *3*, 747.

JP8018606